Journal of Statistical Physics, Vol. 108, Nos. 5/6, September 2002 (© 2002)

Sinai Billiards, Ruelle Zeta-functions and Ruelle Resonances: Microwave Experiments

S. Sridhar[1] **and W. T. Lu**[1]

Received November 6, 2001; accepted March 14, 2002

We discuss the impact of recent developments in the theory of chaotic dynamical systems, particularly the results of Sinai and Ruelle, on microwave experiments designed to study quantum chaos. The properties of closed Sinai billiard microwave cavities are discussed in terms of universal predictions from random matrix theory, as well as periodic orbit contributions which manifest as "scars" in eigenfunctions. The semiclassical and classical Ruelle zeta-functions lead to quantum and classical resonances, both of which are observed in microwave experiments on *n*-disk hyperbolic billiards.

KEY WORDS: Microwave; hyperbolic; Sinai billiard; correlation; Ruelle zeta-function; resonances.

1. INTRODUCTION

It may come as a pleasant surprise to the dynamical systems community, to learn that the work of Yasha Sinai and David Ruelle has had a major impact in experiments on microwave geometries. The connections arise from recent developments which demonstrate that wave mechanics experiments using microwaves are an ideal laboratory for studying the so-called quantum-classical correspondence, a central issue in quantum chaos. These microwave experiments have shown that several theoretical results on the mathematics of chaotic dynamical systems have manifestations in their corresponding quantum or wave mechanics.

The term chaos often means hyperbolicity which guarantees the decomposition of the tangent space at each phase space point into expansion and contraction subspaces. A systematic study of hyperbolic systems

[1] Department of Physics, Northeastern University, Boston, Massachusetts 02115; e-mail: srinivas@neu.edu, wtlu@neu.edu

0022-4715/02/0900-0755/0 © 2002 Plenum Publishing Corporation

from the geometric theory perspective was initiated by Smale.[1] Another viewpoint, namely the ergodic theory or the probability approach, was pioneered by Sinai and Ruelle. Of great interest and possible experimental realization are billiard systems which are two-dimensional, bounded or open. Not all closed billiards have hyperbolic properties. For a dispersing billiard which is closed and has finite concave boundaries, Sinai[2] proved that the system is ergodic. But certain billiards with convex boundaries[3] such as the Bunimovich stadium,[4] were also found to be hyperbolic. Another important billiard system is that of n disks on a plane, which is hyperbolic and a paradigm model of Axiom A systems considered by Ruelle[5] and Pollicott.[6]

Experiments utilizing thin 2-D microwave structures have been shown recently to provide an ideal laboratory system to explore issues in hyperbolic dynamics and quantum chaos. These experiments utilize thin geometries in which Maxwell's equations reduce to the time-independent Schrödinger equation $(\nabla^2 + k^2)\,\Psi = 0$, where Ψ is E_z the z-component of the electric field. This mapping enables precision room temperature experiments exploring wave mechanics on laboratory length scales that can be easily manipulated. The experiments typically probe the two-point Green's function of geometries which may be *closed*, such as the Sinai billiard, or *open*, such as n disks on a plane. In addition to yielding eigenvalue or resonance spectra, a unique advantage of the microwave experiments is the ability to directly map eigenfunctions and standing wave patterns.

A major theme of work in this area has focussed on the quantum-classical boundary. Some of the principal results that have emerged are the observation of scars,[7] precision tests of random matrix theory (RMT) and non-linear sigma models in chaotic and disordered cavities,[8, 9] observation of localization in disordered billiards,[10] and classical and quantum properties of open systems.[11, 12]

These microwave experiments may also be classified as *experimental mathematics*! A noteworthy example is the work on "Not 'Hearing The Shape' of Drums,"[13] which demonstrated experimentally the exact equivalence of eigenvalues of certain isospectral geometries. The isospectrality is purely a consequence of geometry or combinatorics, and is independent of the dynamics (whether chaotic or regular).

This paper summarizes recent results exemplifying the impact of Sinai and Ruelle's work on the microwave quantum chaos experiments. We first discuss the properties of the eigenvalues and eigenfunctions of Sinai billiard-shaped microwave cavities. We then discuss, in the context of 2-D n-disk billiards, the major role of the Ruelle dynamical zeta-functions in the classical and semiclassical theory of chaotic repellers, and the experimental observation of Ruelle–Pollicott resonances.

2. EXPERIMENTS ON SINAI BILLIARDS

Following the pioneering work of Sinai, the Sinai billiard has become a model geometry exemplifying classical and quantum chaos in a closed system. An experimental realization of the Sinai billiard was first achieved in microwave cavities.[7]

The microwave experiments on Sinai billiard cavities yield the eigenvalue spectra $\{E_n = f_n^2\}$ directly as peaks at frequencies $\{f_n\}$ in the experimental 2-point microwave transmission function $S_{21}(f)$ of the cavity (Fig. 1 (top)). Typically $\sim 600-1000$ eigenvalues can be measured in the experimentally accessible frequency window. The corresponding stick spectrum is then analyzed to yield information on spectral statistics. The approach here closely parallels work in spectra of atomic and nuclear systems,[14] which have been analyzed in terms of RMT. Here we summarize the principal results for the Sinai billiard. The main conclusion is that the eigenvalue and eigenfunction statistics are in good agreement with universal predictions of RMT expected to apply to quantum systems with classically chaotic dynamics.[15] However, sufficiently precise experiments clearly reveal deviations from the universal results due to the presence of marginal unstable "bouncing ball" (b-b) orbits.

The nearest neighbor spacing statistics $P(s)$ for the Sinai billiard spectrum shows the well-known level repulsion $P(s) \to 0$ as the spacing $s \to 0$, a characteristic feature of quantum chaos (Fig. 1 (middle)). Fits to the Brody function $P(s) = As^b \exp(-Bs^{b+1})$, yield a Brody parameter $b = 0.92$, where $b = 1.0$ corresponds to exact agreement with the famous Wigner–Dyson statistic, $P(s) = \frac{\pi s}{2} \exp(-\frac{\pi}{4} s^2)$. This deviation is a small but definite signature of the b-b orbits. More striking manifestations of these orbits can be found in longer range correlations, such as the spectral rigidity $\Delta_3(L)$ (Fig. 1 (bottom)). This quantity for the Sinai billiard shows initial agreement with RMT for small L followed by an essentially linear rise from the weak logarithmic dependence expected. Incorporation of the b-b orbits contributions gives excellent agreement between experimental data and theory.

The eigenfunctions corresponding to each eigenvalue peak are obtained using cavity perturbation techniques described in Ref. 16. Representative eigenfunctions of the Sinai billiard are shown in Fig. 2, and show a fascinating variety of patterns. This is in contrast with the rectangular cavity, obtained from the Sinai billiard by removing the central circular disk, for which each eigenfunction can be labeled by $\{m, n\}$, which arise from the integrability of $\{k_x, k_y\}$. Non-integrability in the Sinai billiard is immediately apparent from the fact that the only quantum number that can be assigned to each eigenfunction is E_n—the lack of integrals of motion

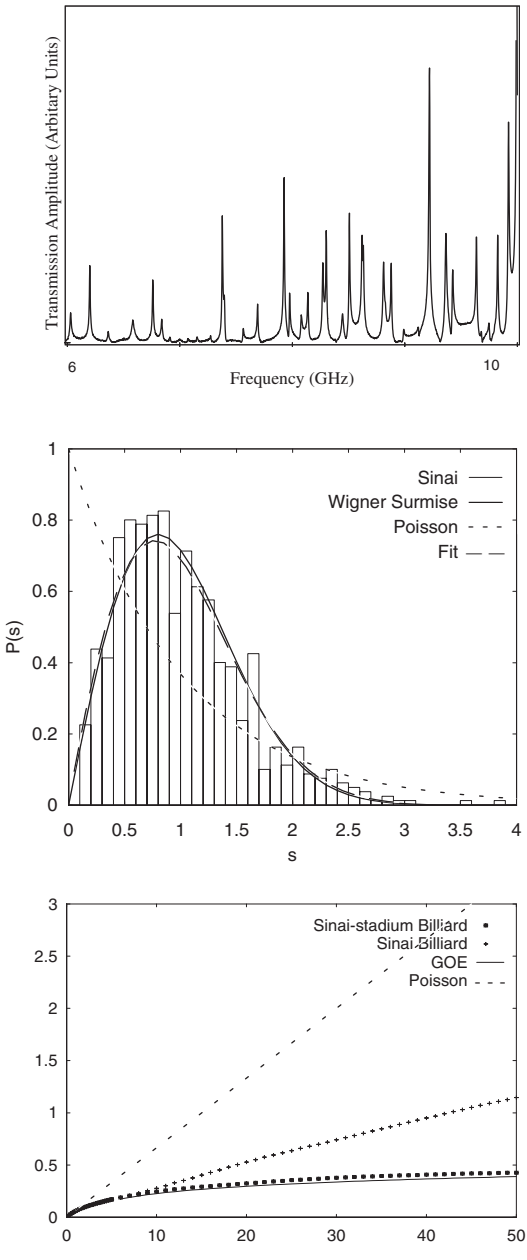

Fig. 1. (Top) Experimental microwave transmission function from a Sinai billiard cavity, (middle) Spacing statistics $P(s)$, (bottom) spectral rigidity $\Delta_3(L)$.

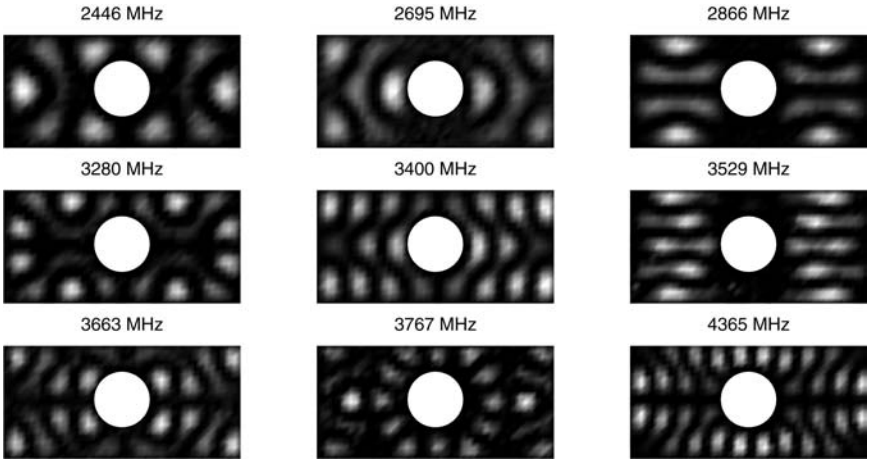

Fig. 2. Representative experimental eigenfunctions of a Sinai billiard microwave cavity. The labels represent corresponding eigenfrequencies.

precludes any further quantum number assignments. The question, what classical phase space structures characterize the eigenfunctions, has occupied physicists for several years. Heller pointed out that the eigenfunctions of chaotic billiards should organize themselves around periodic orbits, even the unstable ones, and called these structures "scars."[17] Scars were seen in numerical simulations, and were implicated indirectly in atomic phenomena. The first direct experimental observation of scars was in eigenfunctions of a Sinai billiard microwave cavity.[7] An example is shown in Fig. 2 at $f = 3663$ MHz. This eigenfunction is scarred along the diagonal periodic orbit, which is unstable. The presence of stable b-b orbits is also visible in some eigenfunctions such as the one at $f = 2866$ MHz. However most of the eigenfunctions are not *visibly* scarred by either stable or unstable PO. A favorite is the one at $f = 3767$ MHz. It shows the circular symmetry of the central disk with almost no visible influence of the rectangular boundary. A more complete characterization of the eigenfunctions in terms of classical phase space structures is a major challenge of research in this area.

Another approach to analyzing eigenfunctions is in terms of their statistical properties. The leading statistic is the density distribution $P(|\Psi|^2)$ which is shown in Fig. 3 (top). For the quarter Sinai billiard, in which the geometric symmetries are absent, the finite probability of finding large densities is evident from the figure. The dependence of $P(|\Psi|^2)$ on the density $|\Psi|^2$ follows closely, but not exactly, the Porter–Thomas (P-T) distribution obtained from RMT. This again is due to the presence of the b-b

orbits. We have confirmed this by showing almost exact agreement with the P-T distribution by removing the b-b orbits by constructing a so-called Sinai stadium, which is a hybrid of the Sinai and stadium billiards.

Spatial correlations $\langle|\Psi(\mathbf{r})|^2\,|\Psi(\mathbf{r}')|^2\rangle$ can also be examined and are shown in Fig. 3 (bottom). The experimental data follow closely the dependence $\langle|\Psi(\mathbf{r})|^2\,|\Psi(\mathbf{r}')|^2\rangle = 1 + cJ_0^2(k\,|\mathbf{r}-\mathbf{r}'|)$, with $c=2$, expected from

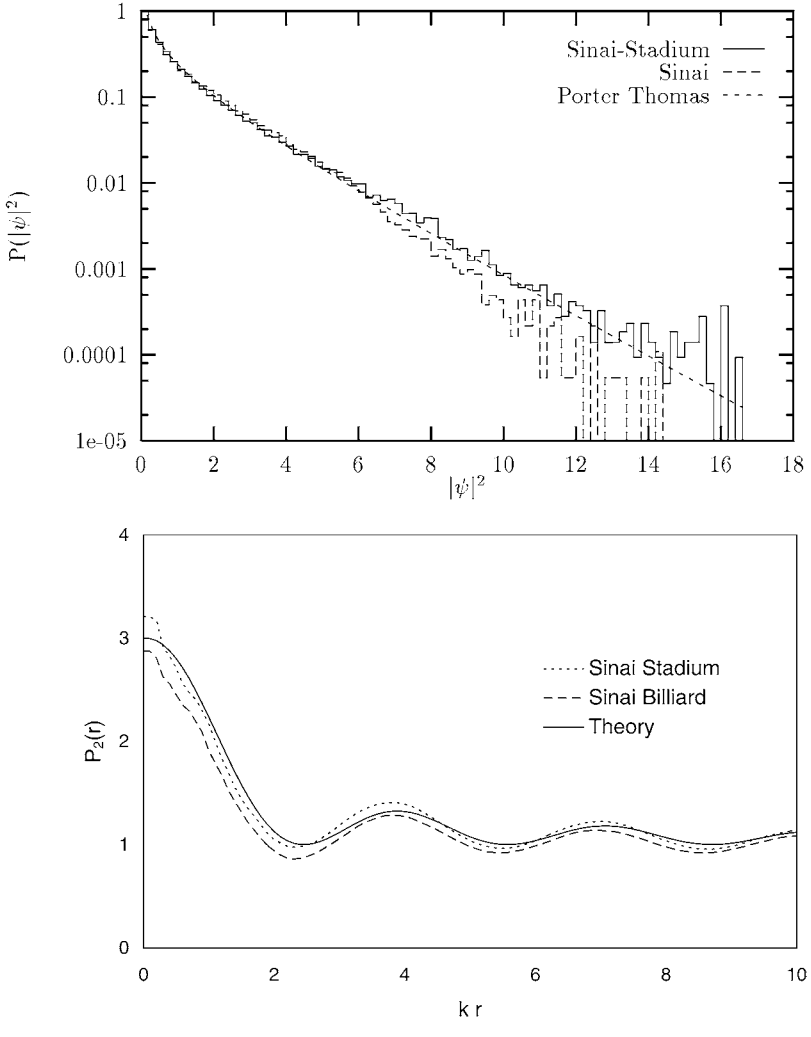

Fig. 3. Statistical properties of eigenfunctions of the Sinai billiard. (top) Density distribution $P(|\Psi|^2)$, (bottom) spatial correlations.

RMT for 2-D. The data for the Sinai billiard lie just below this functional form, this can be seen from the inverse participation ratio $\langle|\Psi(\mathbf{r})|^4\rangle = 2.7 \pm 0.1$, obtained from the spatial correlation with $\mathbf{r} = \mathbf{r}'$. The deviation from the universal value of 3.0 on the lower side is due to the b-b orbits. Here again better agreement with the RMT universal value and function is obtained by eliminating the b-b orbits such as in the Sinai stadium.

In summary the Sinai billiard has been a model system exemplifying the fundamental properties of a quantum chaotic system, with near perfect agreement with RMT predictions for universal distributions of spectral and eigenfunction statistics, and where the deviations from universality are clearly identifiable as arising from b-b orbits.

3. RUELLE ZETA-FUNCTIONS AND RUELLE-POLLICOTT RESONANCES IN *N*-DISK CHAOTIC BILLIARDS

The system of n disks on a plane[18] provides us with a paradigm model system for classical and quantum chaos in open systems. The system is hyperbolic and not ergodic. The microwave realization of the n-disk system is similar to that of the Sinai billiard. To make the system open, microwave absorbers were placed around and far from the disks to have experimentally ignorable reflection, and to provide a good realization of escape to infinity. Because of the C_{nv} symmetry of the n-disk system, one can probe the system in many different ways. Periodic orbit based treatments have been successfully used both classically and semi-classically. The Ruelle dynamical zeta-function, in both the classical and semiclassical versions, has played a major role in studying the properties of this system.

The semiclassical Ruelle zeta-function is

$$\zeta_{\mathrm{sc},j}(-ik) = \prod_p \left(1 - \frac{e^{i(kL_p + \pi\mu_p/2)}}{\sqrt{|\Lambda_p|}\,\Lambda_p^j}\right)^{-1}$$

and the classical Ruelle zeta-function is

$$\zeta_{\mathrm{cl},\beta}(s) = \prod_p \left(1 - \frac{e^{-sT_p}}{|\Lambda_p|\,\Lambda_p^{\beta-1}}\right)^{-1}.$$

The product is over all classical primitive periodic orbits without repetition. Here L_p and T_p are the length and period of periodic orbit p with the Maslov index μ_p. Λ_p is the bigger eigenvalue of the monodromy stability matrix for billiard systems.

The semiclassical Ruelle zeta-function can be derived from the Gutzwiller trace formula[19] of the Green's function in the semiclassical limit $\hbar \to 0$ which is summed over all classical periodic orbits. The finite

widths of the quantum resonances arise in the n-disk system because the system is open and the strange repeller made of classical orbits can trap waves only for finite time. The classical Ruelle zeta-function can be derived from the trace of the resolvent $(s-\mathscr{L})^{-1}$ with $\mathscr{L}f \equiv \{H, f\}$ for Hamiltonian system. For integrable system, the poles of the resolvent operator are purely imaginary, this gives the periodic motion of the classical dynamics. For open or ergodic system, these poles may have nonzero real part and some of them may be real. This gives rise to the correlation decay of the classical dynamics.[20] These complex poles are the Ruelle–Pollicott (R-P) resonances.[5, 6] If the poles are isolated, the decay is exponential. In the case of a branch cut, the decay may be algebraic. Contrary to the trace formula of the classical resolvent[21] which is exact, the semiclassical trace formula of Gutzwiller is not, and it is not always guaranteed that the poles of the semiclassical Ruelle zeta-function are also the poles of the Green's function. But for hard wall systems such as the billiards, the discrepancy was found to be very small.[22, 23] The index j and β comes in from the decomposition of the trace formulas into Ruelle zeta-functions with $j=0, 1,\ldots$ and $\beta=1, 2,\ldots$. One may extrapolate β from integers to real numbers to get more information of the classical dynamics.[24] For the calculation of sharp resonances, only $j=0$ and $\beta=1$ will be needed in the Ruelle zeta-functions.

For the n-disk system, since the velocity of the particle is constant, $L_p = vT_p$, one can simply set $v=1$, and work in the k-space for both the classical and semiclassical Ruelle zeta-functions. If the separation of the disks are big enough to have no tangent orbits, the dynamics is continuously hyperbolic and stable. A symbolic dynamics of $n-1$ symbols with finite grammar exists for the system. The Euler product of the Ruelle zeta-functions can be expanded as $\zeta^{-1} = \prod_p (1-t_p) = 1-\sum_f t_f + \sum_r c_r$. Here t_f is the weight of fundamental orbits f, c_r is the curvature which is the weight difference between long orbit and combination of shorter ones. Only a few primitive POs will be needed in the Ruelle zeta-function to give quite accurate calculation of the poles because the curvature in the cycle expansion will decay exponentially with increasing PO length.[25] This further simplifies the task of calculating resonances. For the 3-disk system, the number of fundamental orbits is just 2. Only 8 periodic orbits with period up to 4 were be needed in the Ruelle zeta-functions to give very accurate estimate of the quantum and classical resonances.

A typical trace of the transmission $T(k) = |S_{21}(k)|^2$ of the quantum resonances is shown in Fig. 4 for the 3-disk system in the fundamental domain. The experimental trace was fitted well by the sum of Lorentzians

$$T(k) = \sum_n \frac{b_n}{(k-s_n)^2 + s_n'^2}.$$

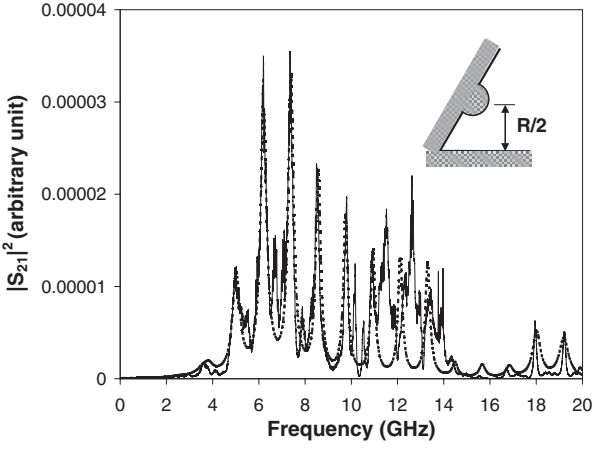

Fig. 4. Quantum resonances of the 3-disk system in the fundamental domain with the distance between the center of the disk of radius 5 cm to the corner being 20 cm. The dashed line uses the semiclassical resonances calculated from the semiclassical Ruelle zeta-function.

Here $s_n + is'_n$ are the semiclassical resonances obtained through the semiclassical Ruelle zeta-function. The coupling b_n depend on the probes location and were chosen to optimize the fitting.

The similarity between the classical Ruelle zeta-function and the semiclassical ones is not coincidental. This implies a deeper relation between the quantum and the classical dynamics besides the correspondence principle. There is increasing interest in understanding the nature of the classical-quantum correspondence. The quantum dynamics is found to approach the classical dynamics with increasing coarse-graining in the phase space for a mixed phase space system.[26] The autocovariance of the two-level spacing and the correlation of the density of states are also found to be related to the classical zeta-function in the study of the Riemann zeta-function zeroes.[27] For an open hyperbolic system, we have shown that the correlation decay of the quantum system is determined by the classical dynamics.[12] That means the classical R-P resonances display their fingerprints in the quantum dynamics. We find that the autocorrelation of the transmission $C(\kappa) = \langle T(k)\, T(k+\kappa)\rangle$ are well-described as a sum of Lorentzians

$$C(\kappa) = \sum_{i,\pm} \frac{c_i}{(\kappa \pm \gamma'_i)^2 + \gamma_i^2}$$

Here $\gamma_i \pm i\gamma'_i$ are the *classical* R-P resonances. The coefficients c_i are related to the eigenfunctions of the Perron–Frobenius operator. The experimental observation of the R-P resonances is illustrated in Fig. 5.

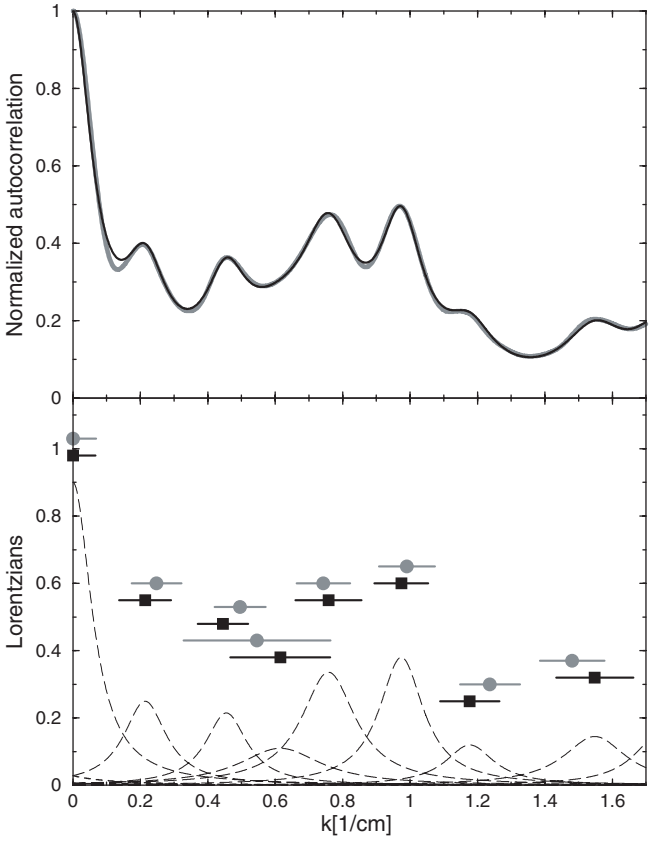

Fig. 5. R-P resonances of the 3-disk system. (top) The experimental autocorrelation $C(\kappa)$ (solid line) and the fitting (gray line). (bottom) Dashed line is the decomposition of $C(\kappa)$ into Lorentzians. Squares with bars are the experimental R-P resonances. Filled circles with bars are R-P resonances calculated from classical Ruelle zeta-function.

We are thus able to observe both the quantum and classical resonances in the same microwave experiment! This exactly parallels the periodic orbit treatment, in which the poles of the semiclassical Ruelle zeta-function yields the quantum resonances while the classical Ruelle zeta-function provides the classical resonances for the hyperbolic n-disk system. The convergence of experiment and theory have been made possible by extensive developments in the machinery of both approaches. The advantages of the microwave experiments are the well-specified nature of the hard wall potentials, and the efficient ensemble averaging that can be achieved. The microwave experiments thus have emerged as an ideal

laboratory system to study both quantum and classical chaos, and some of the mysteries of the quantum-classical correspondence.

In closing, we express our appreciation of the influential role played by the Statistical Physical Workshops at Rutgers University organized by Professor Joel Lebowitz. Our observation of scars in Sinai billiard cavities was first reported at the 1991 meeting, and the observation of R-P resonances was reported in the 2000 meeting.

ACKNOWLEDGMENTS

This work was supported by NSF-PHY-0098801.

REFERENCES

1. S. Smale, *Bull. Amer. Math. Soc.* **73**:747 (1967).
2. Ya. Sinai, *Russian Math. Surveys* **25**:137 (1970).
3. M. Wojtkowski, *Comm. Math. Phys.* **105**:391 (1986).
4. L. A. Bunimovich, *Comm. Math. Phys.* **65**:295 (1979).
5. D. Ruelle, *Phys. Rev. Lett.* **56**:405 (1986); *J. Stat. Phys.* **44**:481 (1986).
6. M. Pollicott, *Ann. Math.* **131**:331 (1990).
7. S. Sridhar, *Phys. Rev. Lett.* **67**:785 (1991).
8. A. Kudrolli, S. Sridhar, A. Pandey, and R. Ramaswamy, *Phys. Rev. E* **49**:R11 (1994).
9. P. Pradhan and S. Sridhar, *Phys. Rev. Lett.* **85**:2360 (1995).
10. A. Kudrolli, V. Kidambi, and S. Sridhar, *Phys. Rev. Lett.* **75**:822 (1995).
11. W. Lu, M. Rose, K. Pance, and S. Sridhar, *Phys. Rev. Lett.* **82**:5233 (1999); W. Lu, L. Viola, K. Pance, M. Rose, and S. Sridhar, *Phys. Rev. E* **61**:3652 (2000).
12. K. Pance, W. Lu, and S. Sridhar, *Phys. Rev. Lett.* **85**:2737 (2000); W. T. Lu, K. Pance, P. Pradhan, and S. Sridhar, *Phys. Scrip.* **T90**:238 (2001).
13. S. Sridhar and A. Kudrolli, *Phys. Rev. Lett.* **72**:2175 (1994).
14. T. Guhr, A. Müller-Groeling, and H. A. Weidenmüller, *Phys. Rep.* **299**:189 (1998).
15. H.-J. Stockmann, *Quantum Chaos: An Introduction* (Cambridge University Press, 1999).
16. S. Sridhar, D. Hogenboom, and B. A. Willemsen, *J. Stat. Phys.* **68**:239 (1992).
17. E. J. Heller, *Phys. Rev. Lett.* **53**:1515 (1984).
18. P. Gaspard and S. A. Rice, *J. Chem. Phys.* **91**:2225, 2242, 2255 (1989).
19. M. C. Gutzwiller, *Chaos in Classical and Quantum Mechanics* (Springer, 1990).
20. L.-S. Young, *Notices of the AMS* **45**:1318 (1998); *Ann. Math.* **147**:585 (1998).
21. P. Cvitanović and B. Eckhardt, *J. Phys. A* **24**:L237 (1991).
22. P. Gaspard, D. Alonso, T. Okuda, and K. Nakamura, *Phys. Rev. E* **50**:2591 (1994).
23. P. Cvitanović, R. Artuso, R. Mainieri, G. Tanner, and G. Vattay, *Classical and Quantum Chaos*, `www.nbi.dk/ChaosBook/` (Niels Bohr Institute, Copenhagen, 2001).
24. P. Gaspard, *Chaos, Scattering, and Statistical Mechanics* (Cambridge University Press, 1998).
25. P. Cvitanović and B. Eckhardt, *Phys. Rev. Lett.* **63**:823 (1989).
26. C. Manderfeld, J. Weber, and F. Haake, *J. Phys. A* **34**:9893 (2001).
27. O. Bohigas, P. Leboeuf, and M. J. Sanchez, *Found. Phys.* **31**:489 (2001).